J Gastroenterol (2021) 56:125–138
https://doi.org/10.1007/s00535-020-01744-1

The Japanese Society of Gastroenterology

ORIGINAL ARTICLE—ALIMENTARY TRACT

Circular RNA TMEM87A promotes cell proliferation and metastasis of gastric cancer by elevating ULK1 via sponging miR-142-5p

Haixiao Wang[1,3] · Guangli Sun[1] · Penghui Xu[1] · Jialun Lv[1] · Xing Zhang[1] · Lu Zhang[1] · Sen Wang[1] · Jiacheng Cao[1] · Yiwen Xia[1] · Zhe Xuan[1] · Bowen Li[1] · Xiaoxu Huang[1] · Tianlu Jiang[1] · Lang Fang[1] · Zekuan Xu[1,2]

Received: 8 July 2020 / Accepted: 20 October 2020 / Published online: 6 November 2020

Abstract

Background Circular RNAs (circRNAs) act as vital regulators of gene expression in a variety of cancers. However, the role of circRNAs in gastric cancer (GC) remains largely unexplored. Herein, we identified that circTMEM87A sponges miR-142-5p to promote GC progression through up-regulating ULK1 expression.

Methods The expression of circTMEM87A in GC was determined by RNA sequencing and quantitative real-time PCR (qRT-PCR). The effects of knockdown or exogenous expression of circTMEM87A on GC cell phenotypes were evaluated both in vitro and in vivo. The interacting miRNA of circTMEM87A was predicted by bioinformatics and confirmed by RNA pull-down, dual-luciferase reporter assay and fluorescence in situ hybridization (FISH). The mechanism by which circTMEM87A/miR-142-5p/ULK1 axis promotes GC was determined by western blot, GFP/mRFP-LC3 puncta analysis, transmission electron microscope (TEM).

Results CircTMEM87A was dramatically elevated in GC tissues and cell lines, and high circTMEM87A expression was closely correlated with poor prognosis of GC patients. Knockdown of circTMEM87A suppressed cell growth, migration, invasion and induced apoptosis in vitro, as well as inhibited GC tumorigenicity and lung metastasis potential in vivo. Meanwhile, circTMEM87A overexpression had the opposite effects. Furthermore, we demonstrated that circTMEM87A could act as a sponge of miR-142-5p to regulate ULK1 expression and GC progression.

Conclusions Our findings suggest that circTMEM87A functions as an oncogene through the miR-142-5p/ULK1 axis in GC. CircTMEM87A might be a prognostic biomarker as well as a promising therapeutic target for GC.

Keywords CircTMEM87A · ULK1 · Gastric cancer · Proliferation · Metastasis

Abbreviations

GC	Gastric cancer
circRNA	Circular RNA
qRT-PCR	Quantitative real-time PCR
FISH	Fluorescence in situ hybridization
RBP	RNA binding protein
miRNA	MicroRNA
3′-UTR	3′-Untranslated region
ULK1	Unc-51 like autophagy activating kinase
OS	Overall survival
siRNA	Small interference RNA
EdU	5-Ethynyl-2′-deoxyuridine
Mut	Mutant
WT	Wild-type
TMEM87A	Transmembrane protein 87A

Haixiao Wang, Guangli Sun and Penghui Xu are contributed equally to this work.

Electronic supplementary material The online version of this article (https://doi.org/10.1007/s00535-020-01744-1) contains supplementary material, which is available to authorized users.

✉ Zekuan Xu
xuzekuan@njmu.edu.cn

[1] Department of General Surgery, The First Affiliated Hospital of Nanjing Medical University, Nanjing 210029, Jiangsu, China

[2] Collaborative Innovation Center For Cancer Personalized Medicine, Nanjing Medical University, Nanjing 210029, Jiangsu, China

[3] Department of General Surgery, The Affiliated Huaian No.1 People's Hospital of Nanjing Medical University, Huaian 223300, Jiangsu, China

EMT	Epithelial to mesenchymal transition
IHC	Immunohistochemistry
HE	Hematoxylin–eosin
NGS	Next-generation sequencing
TEM	Transmission electron microscope

Introduction

Gastric cancer (GC) represents one of the most common malignancies accounting for over 700,000 deaths worldwide each year [1]. Nearly half of the GC patients are in China [2]. In the past few years, although advances in diagnosis approaches and treatment strategies have achieved, the 5-year survival rate of GC patients still remained low [3, 4]. Hence, identification of the molecular mechanisms underlying tumorigenesis of GC is essential for better diagnosis and treatment for GC patients.

Circular RNAs (circRNAs) are a novel class of non-coding endogenous RNAs, featured by a closed loop [5]. CircRNAs are derived from back-splicing of precursor mRNA transcripts and they are conserved and stable owing to its special structure [6–8]. With the development of next-generation sequencing (NGS), an increasing number of circRNAs have been identified [9, 10]. Emerging evidence showed circRNAs play important roles in many physiological and pathophysiological processes, such as aging, tumorigenesis and cardiac hypertrophy [11, 12]. CircRNAs can not only act as RNA binding protein (RBP) sponges [12] but also microRNA (miRNA) sponges [13] which is the commonly reported role of circRNAs in tumorigenesis and progression. CircMTO1 has been reported to sponge miR-9 to inhibit cell proliferation and invasion in human hepatocellular carcinoma [14]. CircRNA_100290 functions a sponge of miR-29 family in oral cancer [15]. CircCCDC66 contributes to colon cancer progression and metastasis by noncoding effects [16].

MiRNAs are small non-coding RNAs which could regulate target mRNA expression by binding to its 3′-untranslated region (3′-UTR) [17]. Previous studies have demonstrated that miRNAs are implicated in many biological and pathological processes, including tumor progression [18, 19]. MiR-142-5p has been confirmed to suppress tumor metastasis by regulating CYR61 expression in GC [20]. MiR-142-5p has also been demonstrated to inhibit tumorigenesis in non-small cell lung cancer [21].

As known, autophagy is a degradation system that transfers cytoplasmic components and organelles to lysosomes to produce energy for cellular renovation and homeostasis [22]. In addition, autophagy has a promotive influence on tumor progression and maintenance via providing materials and energy for cancer cells to overcome nutrient insufficiency and hypoxia [23, 24]. Unc-51 like autophagy activating kinase (ULK1) has been verified to be a vital component of the autophagy pathway [25]. ULK1 has also been identified to be positively correlated with T classification and tumor recurrence of GC patients, and ULK1 overexpression could further accelerate GC cell growth and survival [26].

In our study, circTMEM87A is up-regulated in GC tissues compared with matched normal tissues. We also found that circTMEM87A sponges miR-142-5p to regulate ULK1 expression, and further promotes GC progression. CircTMEM87A might be a new target for the treatment of GC.

Methods

All the methods were included in Electronic Supplementary Material (Online Resource 1).

Results

CircTMEM87A is up-regulated in GC tissues and cells, and high circTMEM87A expression is correlated with poor prognosis of GC patients

To screen the circRNAs involved in GC progression, we employed high-throughput circRNA sequencing (circRNA-seq) to analyze the expression profile of circRNAs in three paired GC tissues and adjacent non-tumorous tissues. We detected a total of 23,029 circRNAs expressed in one or

Fig. 1 circRNA is up-regulated in human GC and characterization of circTMEM87A in GC cell lines. **a** The heat map of high-throughput circRNA sequencing showed the top 30 differentially expressed circRNAs in three paired GC tissues (T) and adjacent normal tissues (N). **b** The volcano map showed the expression variations of these circRNAs in tumorous tissues compared to matched adjacent normal tissues. **c**, **d** The expression levels of circTMEM87A in additional 60 paired GC samples and GC cell lines were measured by qRT-PCR. GAPDH was used to normalize the expression data. **e** GC patients with high circTMEM87A expression ($n = 30$) had a significantly worse 3-year OS compared with patients with low circTMEM87A expression ($n = 30$) using the Kaplan–Meier method ($P < 0.05$). **f** CircTMEM87A is derived from back-splicing of exons 2, 3, 4 and 5 of *TMEM87A* gene. The back-splicing site of circTMEM87A was verified by Sanger sequencing. Red arrow represents the special splicing junction of circTMEM87A. **g** PCR analysis for circTMEM87A and linear TMEM87A in cDNA and gDNA. **h** RNase R assay to analyse the stability of circTMEM87A. qRT-PCR quantified the abundance of circTMEM87A and linear TMEM87A mRNA in BGC823 and MKN45 cells with or without RNase R. **i** Actinomycin D assay to analyse the stability of circTMEM87A. qRT-PCR quantified the expressions of circTMEM87A and TMEM87A mRNA in BGC823 and MKN45 cells treated with or without Actinomycin D at the indicated time points. **j** CircTMEM87A was predominately localized in the cytoplasm of GC cells by FISH assay. The cytoplasmic circTMEM87A was stained green, and the nuclei were stained blue with DAPI. Data were displayed as mean ± SD of three independent experiments. $*P < 0.05$, $**P < 0.01$, $***P < 0.001$

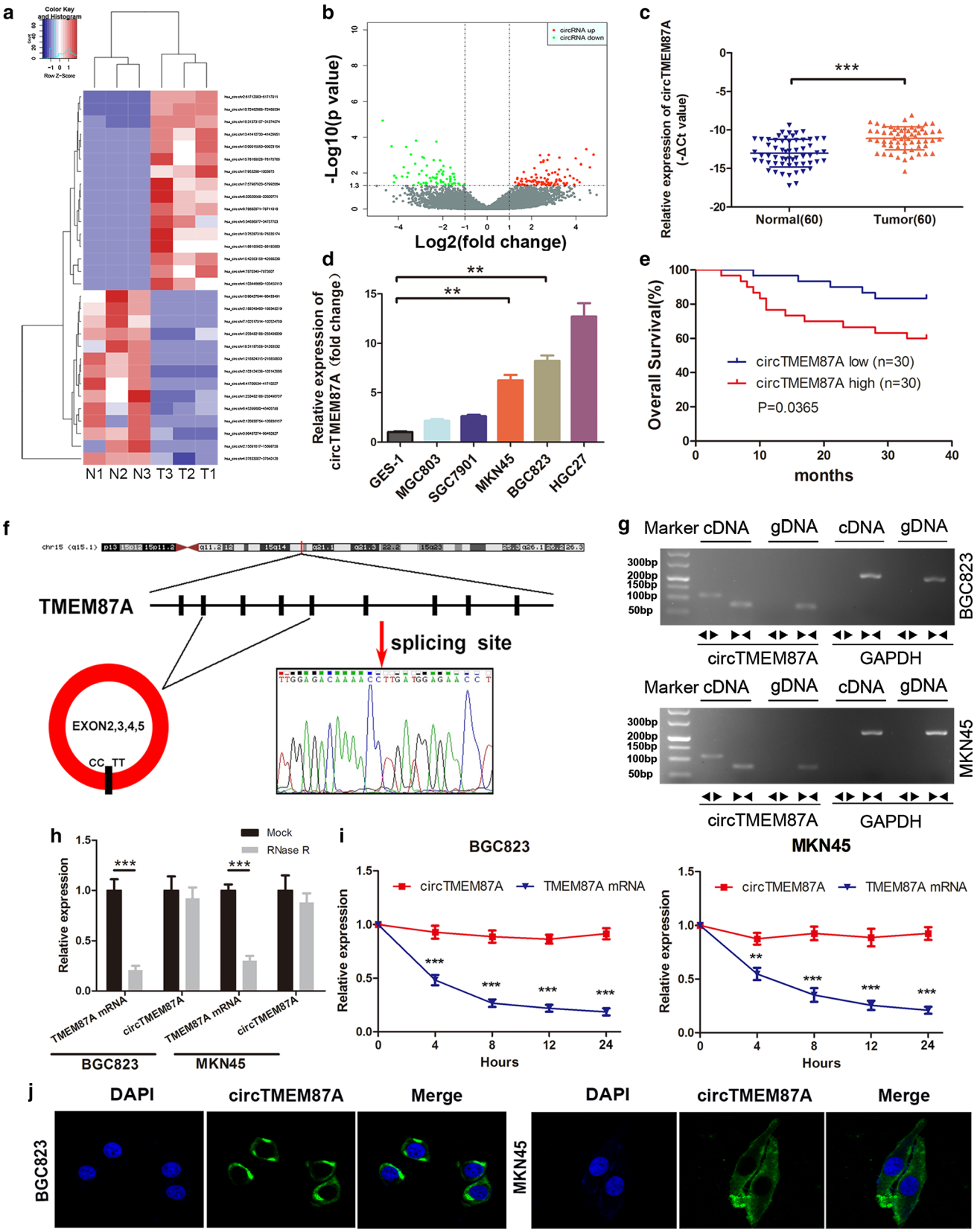
a
Color Key and Histogram
Row Z-Score
N1 N2 N3 T3 T2 T1
b
circRNA up
circRNA down
-Log10(p value)
Log2(fold change)
c
Relative expression of circTMEM87A (-ΔCt value)
***
Normal(60)
Tumor(60)
d
Relative expression of circTMEM87A (fold change)
**
**
GES-1
MGC803
SGC7901
MKN45
BGC823
HGC27
e
Overall Survival(%)
circTMEM87A low (n=30)
circTMEM87A high (n=30)
P=0.0365
months
f
TMEM87A
splicing site
EXON2,3,4,5
CC TT
g
Marker cDNA gDNA cDNA gDNA
300bp
200bp
150bp
100bp
50bp
BGC823
circTMEM87A
GAPDH
MKN45
h
Mock
RNase R
Relative expression
***
***
TMEM87A mRNA
circTMEM87A
TMEM87A mRNA
circTMEM87A
BGC823
MKN45
i
BGC823
MKN45
circTMEM87A
TMEM87A mRNA
Relative expression
Hours
j
DAPI
circTMEM87A
Merge
BGC823
MKN45

more of the samples, including 9999 circRNAs previously reported in circBase. 450 differentially expressed circRNAs were identified, including 314 up-regulated circRNAs and 136 down-regulated circRNAs (fold-change ≥ 2 or ≤ 0.5, $P < 0.05$) (Fig. 1b). A heat map was created showing the top 30 differentially expressed circRNAs in GC tissues relative to matched normal tissues (Fig. 1a). The heat map exhibited that the expression of circTMEM87A (hsa_circ_0034803) was the most significantly increased in GC tissues.

To confirm the results of circRNA-seq, an additional cohort with 60 pairs of GC tissues and adjacent normal tissues were collected to explore the expression of circTMEM87A by quantitative reverse transcription PCR (qRT-PCR). As shown in Fig. 1c, circTMEM87A expression was obviously higher in 81.7% (49 of 60) GC tissues (Fig. 1c, $P < 0.001$). Moreover, we validated the higher levels of circTMEM87A in the HGC27, BGC823, MKN45, SGC7901 and MGC803 gastric cell lines compared with the normal gastric mucosa cell line GES-1 (Fig. 1d). In addition, GC patients with high expression of circTMEM87A had significantly worse 3-year OS than those with lower expression of circTMEM87A ($P = 0.0365$) (Fig. 1e). We also analyzed the relationship between clinicopathological features of the GC patients and circTMEM87A expression level. As shown in supplemental file 1: Table S1, circTMEM87A expression was positively correlated with tumor size and lymph node metastasis. These results suggested that higher circTMEM87A expression may be involved in the pathogenesis of GC.

Characterization of circTMEM87A

Hsa_circ_0034803 (chr15:42,553,155–42,560,230) is derived from exons 2, 3, 4 and 5 regions within transmembrane protein 87A (TMEM87A) locus, so we named it circTMEM87A (Fig. 1f). Sanger sequencing confirmed the genomic sequence of circTMEM87A as in the CircBase database and the head-to-tail splicing (Fig. 1f). To reveal whether the head-to-tail splicing of circTMEM87A results from genomic rearrangements or trans-splicing, cDNA and gDNA of BGC823 and MKN45 cells were extracted. Convergent and divergent primers were designed to amplify circTMEM87A. The results of gel electrophoresis indicated that circTMEM87A could only be amplified by the divergent primers in cDNA, but not in gDNA (Fig. 1g), suggesting that the loop structure of circTMEM87A was derived from reversely splicing. To verify the stability of circTMEM87A, we performed RNAse R resistance assay and confirmed that circTMEM87A, rather than linear TMEM87A, was resistant against digestion of RNAse R in BGC823 and MKN45 cells by qRT-PCR (Fig. 1h). Besides, actinomycin D exposure decreased linear TMEM87A mRNA expression, while it had no effect on circTMEM87A, indicating that circTMEM87A is more stable than linear TMEM87A in BGC823 and MKN45 cells (Fig. 1i). The fluorescence in situ hybridization (FISH) analysis demonstrated that circTMEM87A was predominately distributed in the cytoplasm of GC cells (Fig. 1j).

The expression of circTMEM87A is regulated by QKI

It has been reported that circRNA expression could be regulated by RNA-binding proteins (RBPs), including DExH-Box Helicase 9 (DHX9), adenosine deaminase 1 acting on RNA (ADAR1) and quaking (QKI) [27–29], so we knockdown these three RBPs and observed whether the expression level of circTMEM87A was affected. As shown in Supplementary Fig. 1a–c (Online Resource 2), the results of qRT-PCR revealed that the expression level of circTMEM87A was down-regulated after knockdown of QKI while inhibition of DHX9 or ADAR1 had no effect on the expression level of circTMEM87A. Then we performed IHC on GC and adjacent normal tissues and found QKI was up-regulated in GC tissues (Supplementary Fig. 1d). The results of qRT-PCR also confirmed QKI expression was up-regulated in GC tissues (Supplementary Fig. 1e). To further validate the relationship between QKI and circTMEM87A, we performed linear correlation analysis and found circTMEM87A expression level was positively correlated with QKI expression level in GC tissues (Supplementary Fig. 1f). Taken together, the highly expressed circTMEM87A was, at least partly, caused by up-regulation of QKI in GC.

CircTMEM87A promotes GC cell proliferation and attenuates cell apoptosis in vitro

To determine whether circTMEM87A affects biological behavior of GC cells, we designed a specific small interference RNA (siRNA) to silence the expression of circTMEM87A and constructed a circTMEM87A overexpression vector. As shown in Fig. 2a and

Fig. 2 circTMEM87A promotes cell proliferation and attenuates cell apoptosis in vitro. **a** Expression levels of circTMEM87A and TMEM87A mRNA in BGC823 cells treated with circTMEM87A siRNA or circTMEM87A over-expression plasmids. **b** Cell growth analysis of BGC823 cells after silencing or overexpressing circTMEM87A by CCK8 assay. **c**, **d** Effects of circTMEM87A expression alteration on colony formation and EdU cell proliferation of BGC823 cells. **e** The effect of circTMEM87A on cell apoptosis by Annexin V-FITC apoptosis assay. **f** Transwell migration and invasion assays to assess the effect of si-circTMEM87A or circTMEM87A overexpression on BGC823 cells. **g** The effect of circTMEM87A on apoptosis-related proteins expression. **h** Western blot was applied to measure Snail, TWIST, N-cadherin and E-cadherin protein expression levels in treated BGC823 cells. GAPDH was used as an internal control. The experiment was done in triplicates. $*P < 0.05$, $**P < 0.01$

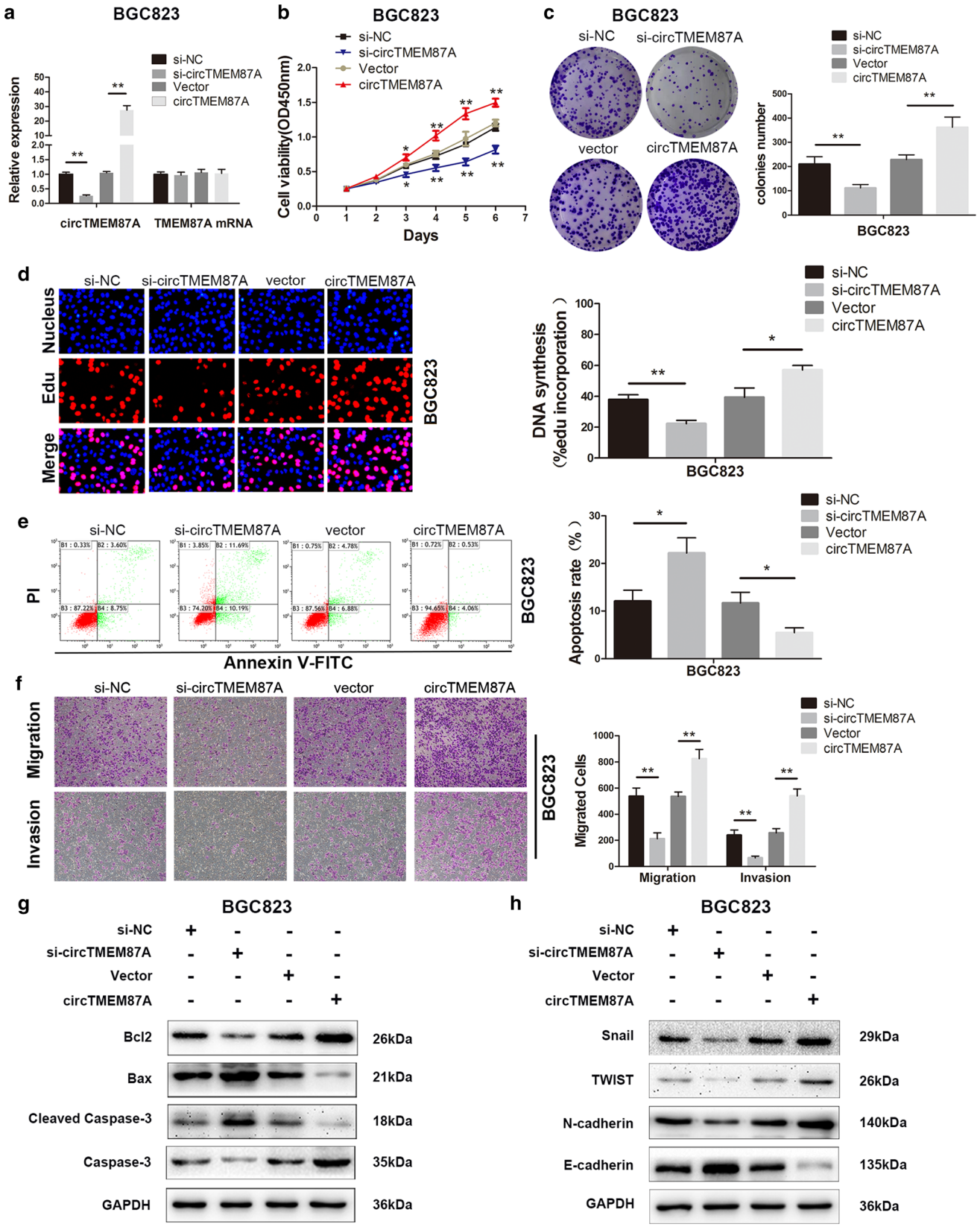
a
BGC823
si-NC
si-circTMEM87A
Vector
circTMEM87A
Relative expression
circTMEM87A
TMEM87A mRNA
b
BGC823
si-NC
si-circTMEM87A
Vector
circTMEM87A
Cell viability(OD450nm)
Days
c
BGC823
si-NC
si-circTMEM87A
vector
circTMEM87A
colonies number
BGC823
d
si-NC
si-circTMEM87A
vector
circTMEM87A
Nucleus
Edu
Merge
BGC823
DNA synthesis (%edu incorporation)
BGC823
e
si-NC
si-circTMEM87A
vector
circTMEM87A
PI
Annexin V-FITC
BGC823
Apoptosis rate (%)
BGC823
f
si-NC
si-circTMEM87A
vector
circTMEM87A
Migration
Invasion
BGC823
Migrated Cells
Migration
Invasion
g
BGC823
si-NC
si-circTMEM87A
Vector
circTMEM87A
Bcl2
Bax
Cleaved Caspase-3
Caspase-3
GAPDH
26kDa
21kDa
18kDa
35kDa
36kDa
h
BGC823
si-NC
si-circTMEM87A
Vector
circTMEM87A
Snail
TWIST
N-cadherin
E-cadherin
GAPDH
29kDa
26kDa
140kDa
135kDa
36kDa

Supplementary Fig. 2a (Online Resource 3), compared with si-NC, si-circTMEM87A effectively knocked down circTMEM87A expression and had no effect on TMEM87A mRNA expression. By transfection of recombinant circTMEM87A plasmid, circTMEM87A was successfully overexpressed in BGC823 and MKN45 cells, with no significant change of TMEM87A mRNA expression (Fig. 2a and Supplementary Fig. 2a). Knockdown of circTMEM87A in BGC823 and MKN45 cells significantly reduced cell proliferation ability and promoted cell apoptosis using CCK8, colony formation assays, EdU, and Annexin V-FITC apoptosis detection assay (Fig. 2b–e and Supplementary Fig. 2b–e). Furthermore, we found that ectopic circTMEM87A expression markedly promoted cell proliferation than the negative control in BGC823 and MKN45 cells (Fig. 2b–d and Supplementary Fig. 2b–d). Flow cytometric assay with Annexin V/FITC exhibited that the cellular apoptotic rate was decreased after circTMEM87A plasmid transfection (Fig. 2e and Supplementary Fig. 2e). These results indicated that circTMEM87A is essential to maintain GC cell growth. To clarify the mechanism by which circTMEM87A affects cell apoptosis, we applied western blot to detect the expression of apoptosis-related proteins, including Bcl2, Bax and cleaved caspase-3. As shown in Fig. 2g and Supplementary Fig. 2g, circTMEM87A silencing enhanced Bax and cleaved caspase-3 protein expression, whereas the expression levels of Bcl2 and the inactivated form of caspase-3 protein were down-regulated. As expected, western blot analysis demonstrated that the protein expression of Bax and cleaved caspase-3 was decreased by circTMEM87A overexpression in BGC823 and MKN45 cell lines compared with the control group, while ectopic expression of circTMEM87A resulted in the up-regulation of Bcl2 and the inactivated form of caspase-3 protein expression.

CircTMEM87A positively regulates migration and invasion of GC cells

Tumor migration and invasion are critical factors affecting the survival of cancer patients. Given that circTMEM87A expression is statistically associated with tumor size and N classification of GC patients (Table S1), circTMEM87A may play a role in metastasis. To verify the hypothesis, the effect of circTMEM87A on cell migration and invasion was evaluated. Si-circTMEM87A was transiently transfected into BGC823 and MKN45 cells to down-regulate the circTMEM87A expression. As shown in Fig. 2f and Supplementary Fig. 2f, knockdown of circTMEM87A inhibited migration and invasion abilities of BGC823 and MKN45 cells while circTMEM87A overexpression had the opposite effect. Epithelial to mesenchymal transition (EMT) is an important event in cancer progression and is closely correlated with GC cell migration and invasion. Thus, we investigated the role of circTMEM87A in the regulation of EMT-related factors. As shown in Fig. 2h and Supplementary Fig. 2h, down-regulation of circTMEM87A availably suppressed the expression of mesenchymal cell marker N-cadherin and transcription factors which include Snail and TWIST but increased the expression of epithelial cell marker E-cadherin. On the contrary, as a result of circTMEM87A overexpression in BGC823 and MKN45 cells, the expression levels of Snail, TWIST and N-cadherin significantly increased, while the epithelial marker E-cadherin decreased. Collectively, these data supported that circTMEM87A accelerates GC cell migration and invasion in the molecular level.

CircTMEM87A acts as a putative miR-142-5p sponge

It is well known that circRNAs which are mainly localized in the cytoplasm rather than nucleus, can exert their biological effects by sponging miRNAs and preventing miRNAs from regulating their target mRNAs. To find the potential target miRNA of circTMEM87A, we firstly performed miRNA sequencing of 3 paired GC tissues and adjacent non-tumorous tissues which were previously used for circRNA sequencing to detect the down-regulated miRNAs in GC (Fig. 3a). Next, we overlapped the prediction results of miRanda (https://microrna.org/microrna/home.do) and TargetScan (https://www.targetscan.org) and miRNA sequencing data. 5 candidate miRNAs were screened out, including miR-561-5p, miR-590-3p, miR-153-3p, miR-142-5p and miR-653-3p (Fig. 3b). To verify

Fig. 3 CircTMEM87A acts as a miRNA-142-5p sponge in GC cell lines. **a** The heat map shows the significantly down-regulated miRNAs in three paired of GC and adjacent normal tissues by miRNA sequencing. **b** Schematic model exhibits the overlap of the target miRNAs of circTMEM87A predicted by miRanda, TargetScan and miRNA sequencing. **c**, **d** CircTMEM87A in BGC823 and MKN45 cell lysates was pulled down and enriched with circTMEM87A specific probe and detected by RT-PCR (**c**) and qRT-PCR (**d**). GAPDH was used as an internal. The relative expression level of circTMEM87A was calculated by normalizing to the input. **e**, **f** The relative expression levels of five candidate miRNAs in BGC823 and MKN45 lysates pulled down by circTMEM87A probe or oligo probe were tested by qRT-PCR. **g** Schematic representation of the potential binding site of miR-142-5p with circTMEM87A. The luciferase activity in BGC823 and MKN45 cells after co-transfection with a luciferase reporter plasmid containing circTMEM87A sequences with wild-type or mutated miR-142-5p binding sites and miR-142-5p mimics or miR-NC. **h**, **i** RNA FISH for miR-142-5p and circTMEM87A was detected in BGC823 and MKN45 cell lines. Nuclei were stained blue (DAPI), circTMEM87A was stained green, and miR-142-5p was stained red. Data are presented as means ± SD. $^{*}P < 0.05$, $^{**}P < 0.01$, $^{***}P < 0.001$

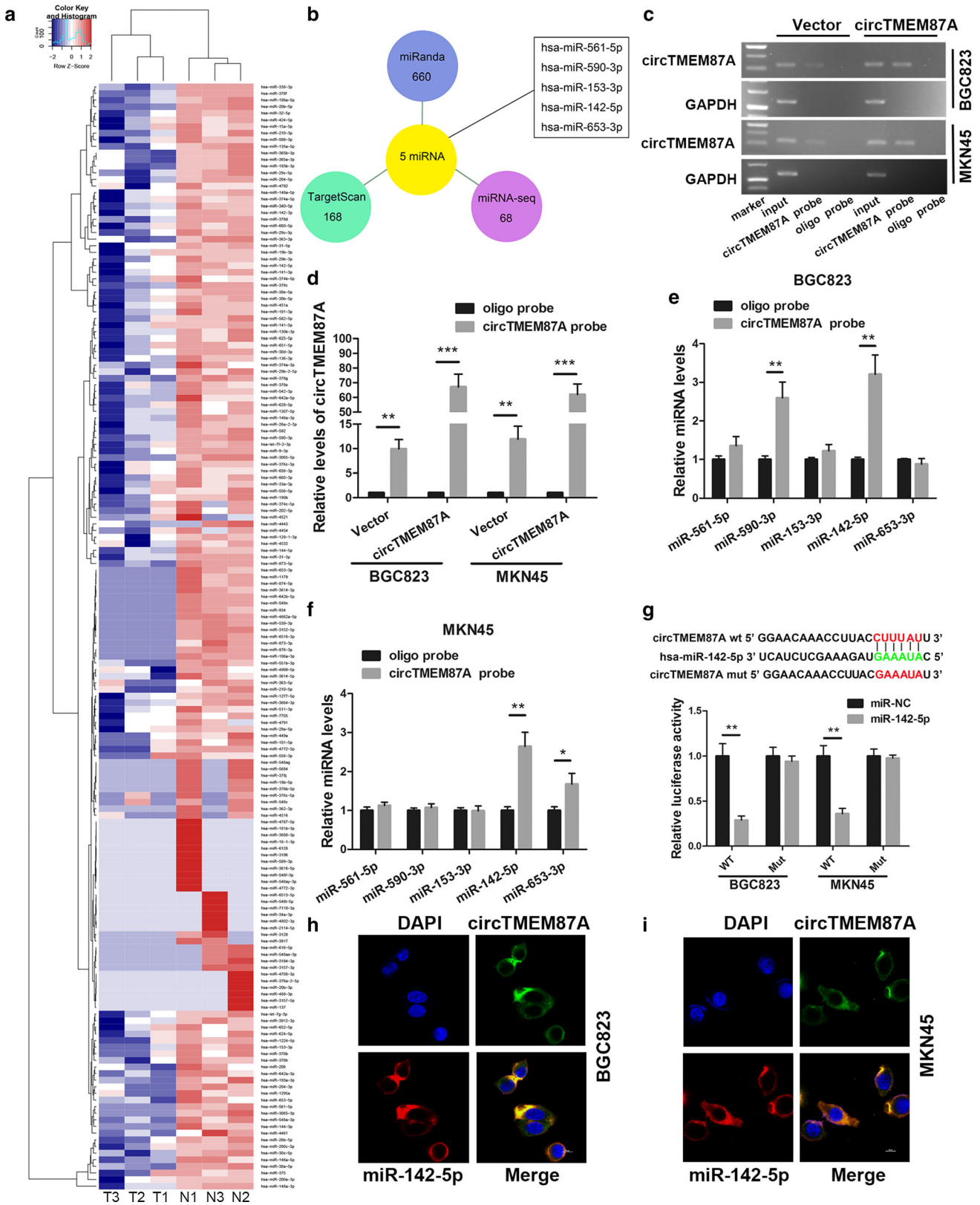
a
Color Key and Histogram
Row Z-Score
T3 T2 T1 N1 N3 N2
b
miRanda 660
5 miRNA
TargetScan 168
miRNA-seq 68
hsa-miR-561-5p
hsa-miR-590-3p
hsa-miR-153-3p
hsa-miR-142-5p
hsa-miR-653-3p
c
Vector circTMEM87A
circTMEM87A
GAPDH
circTMEM87A
GAPDH
BGC823
MKN45
marker input circTMEM87A probe oligo probe input circTMEM87A probe oligo probe
d
oligo probe
circTMEM87A probe
Relative levels of circTMEM87A
Vector circTMEM87A Vector circTMEM87A
BGC823 MKN45
e
BGC823
oligo probe
circTMEM87A probe
Relative miRNA levels
miR-561-5p miR-590-3p miR-153-3p miR-142-5p miR-653-3p
f
MKN45
oligo probe
circTMEM87A probe
Relative miRNA levels
miR-561-5p miR-590-3p miR-153-3p miR-142-5p miR-653-3p
g
circTMEM87A wt 5' GGAACAAACCUUACCUUUAUU 3'
hsa-miR-142-5p 3' UCAUCUCGAAAGAUGAAAUAC 5'
circTMEM87A mut 5' GGAACAAACCUUACGAAAUAU 3'
miR-NC
miR-142-5p
Relative luciferase activity
WT Mut WT Mut
BGC823 MKN45
h
DAPI circTMEM87A
BGC823
miR-142-5p Merge
i
DAPI circTMEM87A
MKN45
miR-142-5p Merge

the interaction between circTMEM87A and candidate miRNAs, we designed a biotin-labeled probe specific for circTMEM87A to pull down circTMEM87A in BGC823 and MKN45 cells. CircTMEM87A was pulled down more abundantly in cells transfected with circTMEM87A overexpression plasmid relative to empty vector (Fig. 3c, d). The expression levels of the 5 candidate miRNAs were detected following pull-down assays. The results of qRT-PCR indicated that miR-142-5p was the only miRNA which was statistically abundant in a pull-down assay with circTMEM87A probe in both BGC823 and MKN45 cells, suggesting that miR-142-5p was interacted with circTMEM87A in GC cells (Fig. 3e, f). To further validate the interaction between miR-142-5p and circTMEM87A, the luciferase reporter assay was performed. The binding site of miR-142-5p to circTMEM87A was exhibited in Fig. 3g. The results showed that miR-142-5p overexpression significantly reduced the luciferase activity of the wild-type LUC-circTMEM87A reporter gene in both BGC823 and MKN45 cell lines. By contrast, the luciferase activity of LUC-circTMEM87A-mutant reporter gene was not declined when co-transfected with miR-142-5p mimics (Fig. 3g). In addition, FISH analysis revealed that circTMEM87A and miR-142-5p were co-localized in the cytoplasm of BGC823 and MKN45 cells (Fig. 3h, i). As shown in Supplementary Fig. 3a (Online Resource 4), miR-142-5p was found to be down-regulated in GC tissues by qRT-PCR. GC patients with high miR-142-5p expression had a significantly better 3-year OS compared with patients with low miR-142-5p expression ($P = 0.0326$) (Supplementary Fig. 3b). The expression level of miR-142-5p was negatively correlated with the expression level of circTMEM87A in GC tissues (Supplementary Fig. 3c). All these results indicated that circTMEM87A acts as a sponge of miR-142-5p in GC.

ULK1 is a target of miR-142-5p

To find out the target gene of miR-142-5p, four databases including miRDB (https://mirdb.org/), TargetScan (https://www.targetscan.org), miRWalk (https://www.ma.uni-heidelberg.de/apps/zmf/mirwalk/), and PicTar (https://pictar.mdc-berlin.de/) were screened and 23 target genes were overlapped in these four databases. We then chose IGF2BP3, ULK1, MCL1 and SOX5 which have been reported to promote GC progression for further analysis (Fig. 4a). qRT-PCR results indicated that ULK1 and MCL1 were significantly up-regulated in both BGC823 and MKN45 cells transfected with miR-142-5p inhibitor compared with those transfected with the negative control NC, implying that ULK1 and MCL1 may be the direct targets of miR-142-5p in GC (Fig. 4b). Bioinformatics analysis predicted a putative 7-mer-binding site with miR-142-5p in the 3′UTR of ULK1 (Fig. 4c) and MCL1 (Supplementary Fig. 4a, Online Resource 5) transcript. To validate whether miR-142-5p directly targets ULK1 or MCL1, dual-luciferase reporter assays were performed. As shown in Fig. 4d, miR-142-5p overexpression significantly decreased the luciferase activity of wild-type ULK1, but had no effect on the mutant ULK1 in GC cells, suggesting that miR-142-5p could specifically bind to the ULK1 3′UTR. However, miR-142-5p overexpression failed to alter the luciferase activity of wild-type MCL1 (Supplementary Fig. 4b). In addition, ectopic overexpression of miR-142-5p was demonstrated to suppress ULK1 mRNA expression by qRT-PCR (Fig. 4e). miR-142-5p overexpression was also observed to inhibit ULK1 protein expression while knockdown of miR-142-5p had the opposite effect (Fig. 4f). Moreover, higher ULK1 expression was correlated with lower overall survival rates in patients with GC according to the public database Kaplan–Meier Plotter (https://kmplot.com/analysis/) (Fig. 4g). As shown in Supplementary Fig. 5a (Online Resource 6), ULK1 was found to be up-regulated in GC tissues by qRT-PCR. The expression level of ULK1 was negatively correlated with the expression level of miR-142-5p in GC tissues (Supplementary Fig. 5b). Based on the above results, ULK1 is a direct target of miR-142-5p. ULK1 expression was found to be positively correlated with circTMEM87A in GC tissues by linear correlation analysis (Supplementary Fig. 5c).

ULK1 reverses the effects of circTMEM87A on GC cells

To further elucidate whether the effects of circTMEM87A on proliferation and metastasis of GC cells were mediated by enhanced expression of ULK1, rescue experiments were performed. We identified that ULK1 overexpression promoted the proliferation and migration of GC cells by EdU, colony formation and transwell migration assays (Fig. 5a, b). Intriguingly, the suppressive effect of circTMEM87A silencing on cell proliferation and migration was abrogated by ULK1 overexpression in both BGC823 and MKN45 cell lines (Fig. 5a, b). The rates of EdU-incorporated positive cells and the number of colonies in different groups were counted and shown in Supplementary Fig. 6a, b (Online Resource 7). ULK1 is a Ser/Thr protein kinase involved in triggering autophagy initiation [30] and is dysregulated in several tumor types, including GC [26]. So we further investigated the roles of circTMEM87A and ULK1 in GC autophagy determined by GFP/mRFP-LC3 puncta analysis and transmission electron microscope (TEM). As shown in Fig. 5c and Supplementary Fig. 7a (Online Resource 8), we found that GFP/mRFP-LC3 puncta accumulation was reduced following circTMEM87A depletion but increased

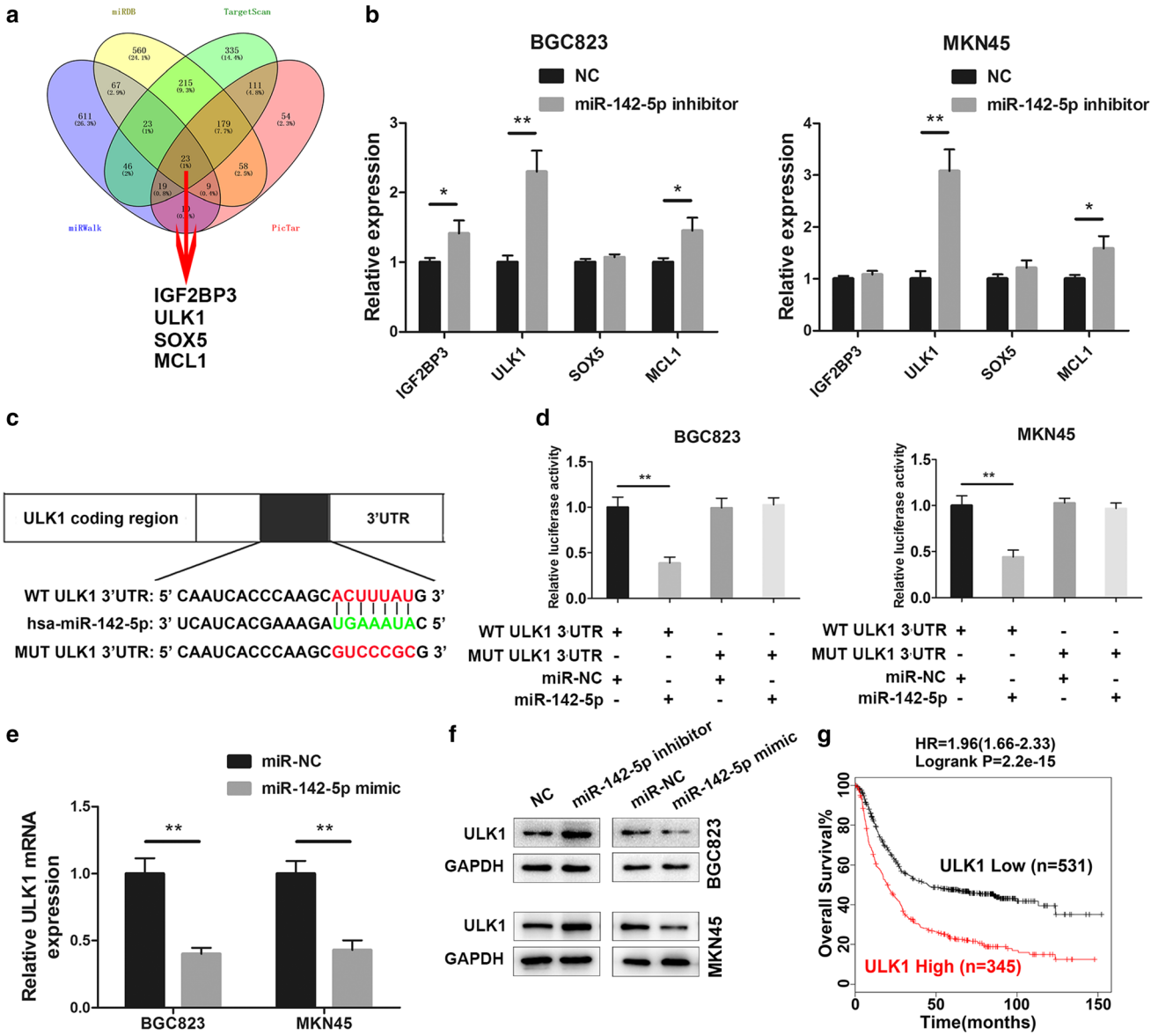

Fig. 4 ULK1 was targeted by miR-142-5p in GC cells. **a** Venn diagram of target genes of miR-142-5p predicted by miRDB, TargetScan, miRWalk, and PicTar. **b** qRT-PCR analysis of the relative levels of the 4 candidate genes in BGC823 and MKN45 cells transfected with miR-142-5p inhibitor or negative control. **c** Schematic illustration of the binding site between miR-142-5p and wild-type (WT) or mutant (Mut) *ULK1* 3′UTR. **d** Relative luciferase activity of WT or Mut *ULK1* 3′UTR in BGC823 and MKN45 cell lines after overexpression of miR-142-5p. **e**, **f** qRT-PCR (**e**) and western blot (**f**) showing the effects of altered miR-142-5p level on ULK1 expression. **g** The survival analysis of ULK1 using online database Kaplan–Meier Plotter

after ULK1 overexpression in GC cell lines. Notably, co-transfection of ULK1 overexpression plasmid in circTMEM87A silencing cells reversed the suppressive effect of si-circTMEM87A in both BGC823 and MKN45 cell lines. Consistent with the above result, the similar roles of circTMEM87A and ULK1 in GC autophagy were observed by TEM (Fig. 5c and Supplementary Fig. 7a). Subsequently, we performed western blot to identify whether circTMEM87A regulate autophagy of GC cells via ULK1. When circTMEM87A was down-regulated, the levels of autophagy-related proteins Beclin 1, LC3II and ULK1 protein expression were dramatically decreased, but the level of P62 protein expression increased. Following ULK1 reconstitution, the effects of circTMEM87A knockdown on the levels of autophagy-related proteins expression were reversed (Fig. 5d). Taken together, we drew the conclusion that circTMEM87A could play an oncogenic role by regulating ULK1 which promoted autophagy.

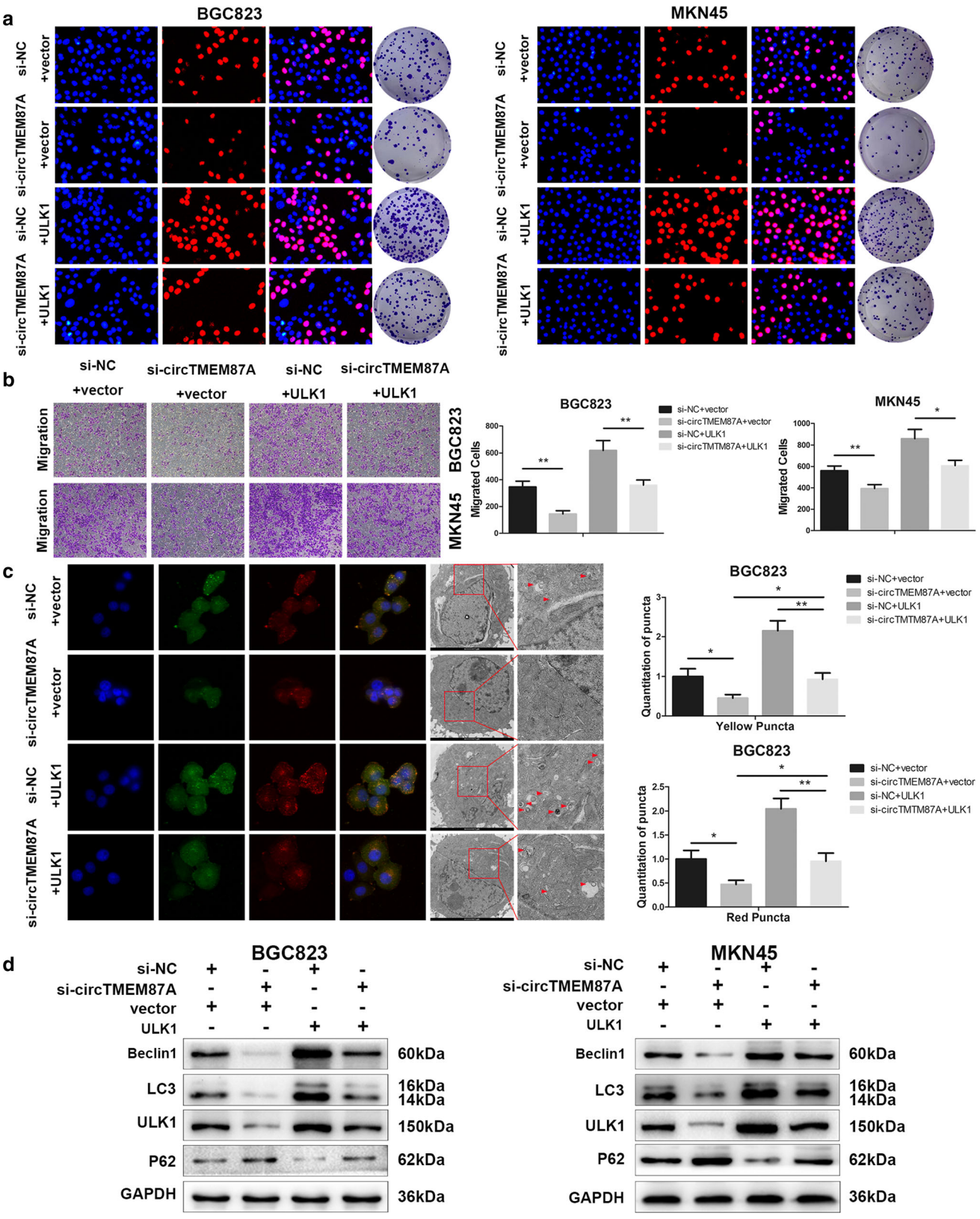
a
BGC823
MKN45
si-NC
+vector
si-circTMEM87A
+vector
si-NC
+ULK1
si-circTMEM87A
+ULK1
b
si-NC
+vector
si-circTMEM87A
+vector
si-NC
+ULK1
si-circTMEM87A
+ULK1
Migration
BGC823
MKN45
Migrated Cells
si-NC+vector
si-circTMEM87A+vector
si-NC+ULK1
si-circTMTM87A+ULK1
c
Quantitation of puncta
Yellow Puncta
Red Puncta
d
si-NC
si-circTMEM87A
vector
ULK1
Beclin1
LC3
ULK1
P62
GAPDH
60kDa
16kDa
14kDa
150kDa
62kDa
36kDa

◀**Fig. 5** ULK1 reverses the oncogenic effects of circTMEM87A silencing on GC cells in vitro. **a** Co-transfection of ULK1 overexpression plasmids in circTMEM87A silencing cells counteracted the suppressing function of si-circTMEM87A in BGC823 and MKN45 cell lines by EdU and colony formation assays. **b** The inhibition of cell migration by circTMEM87A knockdown was restored by ULK1 up-regulation. **c** ULK1 eliminated the role of circTMEM87A on autophagy in GC cells using GFP/mRFP-LC3 puncta analysis and TEM. Yellow puncta represent autophagosomes and red puncta represent autolysosomes. The red arrows refer to cellular autophagosomes or autolysosomes. **d** The expression levels of autophagy-associated proteins were detected with circTMEM87A knockdown or overexpression

CircTMEM87A contributes to tumor growth and metastasis in vivo

To assess the potential role of circTMEM87A in tumor growth in vivo, we subcutaneously injected 1×10^6 GC cells into the flanks of nude mice. Overexpression of circTMEM87A promoted tumor growth while knockdown of circTMEM87A decreased the weight of harvested tumors (Fig. 6a). Then immunohistochemical staining was performed on the implanted tumor tissues from nude mice with anti-ki67 antibody. The ki67 staining results indicated a lower proliferation index in the circTMEM87A knockdown group compared with negative controls, whereas the circTMEM87A-overexpressing group exerted the opposite trend (Fig. 6b). Meanwhile, we also attempted to detect the role of circTMEM87A in tumor metastasis in vivo via injecting stable transfected cells into tail veins of BALB/c nude mice. Lung metastases and peritoneal metastases were observed by detecting luciferase intensities after 4 weeks. Importantly, we found a significant inhibition on lung metastases in circTMEM87A knockdown group compared with the control group while ectopic expression of circTMEM87A promoted lung metastases of GC cells (Fig. 6c). Additionally, lung tissues of nude mice were harvested and examined by hematoxylin–eosin (HE) staining. The results of HE staining showed that the size of metastatic nodules in the lungs was positively associated with circTMEM87A expression level (Fig. 6d). These findings implied that circTMEM87A could facilitate tumorigenesis and metastasis of GC cells in vivo.

Discussion

The number of the patients diagnosed with GC and died of GC every year in China accounted for about half of the cases and deaths all over the world [31], so it is of great necessity to discover new targets for GC treatment. In our study, we first performed NGS on three pairs of GC tissues and matched normal tissues to identify the circRNA profile. Most circRNAs exert their function by sponging miRNAs, others by binding to RNA binding proteins. A few circRNAs even could be translated into proteins or peptides [32]. We first reported the role of circTMEM87A in GC. CircTMEM87A was found to be increased in GC tissues based on the results of qRT-PCR performed on 60 pairs of GC and normal tissues. Inhibition of QKI could decrease expression of circTMEM87A and QKI was also found to be up-regulated in GC tissues by IHC and qRT-PCR. The expression level of circTMEM87A was confirmed to be positively correlated with the expression level of QKI. The highly expressed circTMEM87A was, at least partly, caused by up-regulation of QKI in GC. Prognosis of the patients with higher expression of circTMEM87A is worse according to our follow-up data. The expression of circTMEM87A is positively related to tumor size and lymph node metastasis. These findings suggest that circTMEM87A might play an oncogenic role in GC which needs further mechanism research.

Sanger sequencing was applied to identify the splicing site of circTMEM87A. The results of actinomycin D assay and RNAse R assay proved that the circular form of TMEM87A is more stable than its linear form. CircTMEM87A was demonstrated to promote the proliferation of BGC823 and MKN45 by CCK-8 assay, colony formation assay and EdU assay. The results of annexin V-FITC apoptosis analysis and western blot detecting expression of apoptosis-related proteins revealed that increased circTMEM87A expression could inhibit apoptosis of GC cells. CircTMEM87A could also facilitate migration and invasion ability in a transwell assay. To find out the potential sponge miRNAs of circTMEM87A, we combined the results of miRNA sequencing and online database prediction. Five candidate miRNAs were screened out of which miR-142-5p was then confirmed to be sponged by circTMEM87A with subsequent RNA pull-down assay. We finally carried out luciferase reporter assay and FISH assay to further verify the interaction between circTMEM87A and miR-142-5p. MiR-142-5p was previously reported to involve in a wide spectrum of cancer, including pancreatic cancer [33], colorectal cancer [34], breast cancer [35] and gastric cancer [36, 37]. Based on the prediction results of four online databases and qRT-PCR assay, ULK1 and MCL1 were considered to be the potential targets of miR-142-5p. We then performed luciferase reporter assay to confirm ULK1, rather than MCL1 was a direct target of miR-142-5p. One miRNA can have hundreds of target genes and be involved in multiple biological processes. MiR-142-5p might reduce mRNA level of a certain transcription factor which regulates MCL1 expression. Through this mechanism, miR-142-5p inhibitor could increase MCL1 expression even though MCL1 is not a direct target of miR-142-5p. However, this is just a

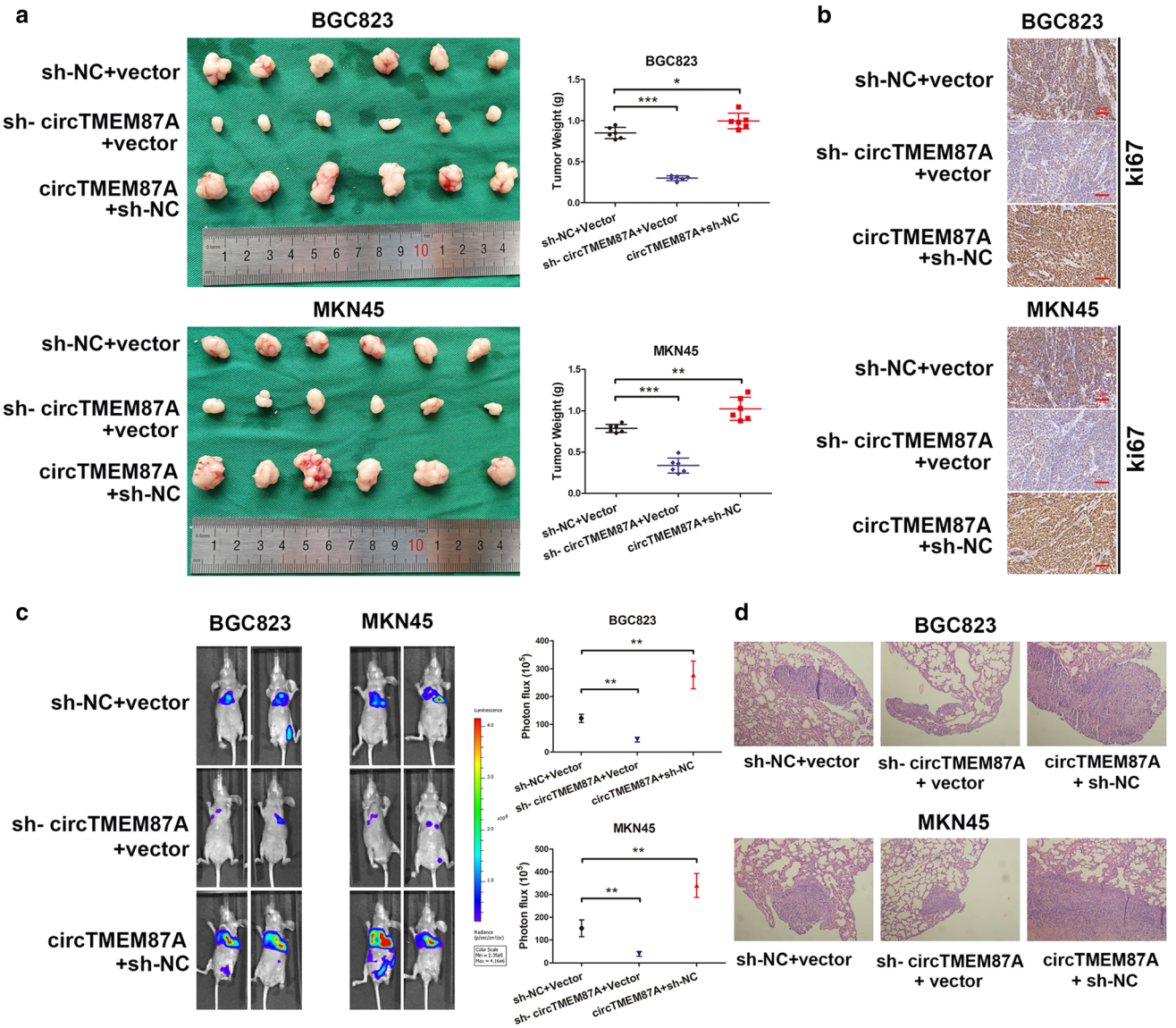

Fig. 6 circTMEM87A promotes tumor growth and metastasis of GC cells in vivo. **a** The volume (Left) and weight (Right) of xenograft tumors in nude mice ($n = 6$) with circTMEM87A knockdown or overexpression 4 weeks after subcutaneously injection with GC cells. **b** Ki-67 staining of GC xenografts in nude mice. **c** In vivo bioluminescence imaging shows tumors in nude mice 4 weeks after injection with GC cells. The color scale bar represents the photon flux (p/s) emitted from the nude mice. Luciferase intensities were detected in the thoracic cavity of different animal groups. **d** Representative pictures of HE staining of metastatic nodules in the lungs of different animal groups. $^{*}P < 0.05$, $^{**}P < 0.01$, $^{***}P < 0.001$

hypothesis and we will try to validate it in further research. ULK1 is a kind of kinase which could induce autophagy [38]. ULK1 expression is negatively correlated with overall survival of GC patients according to Kaplan Meier-plotter. Rescue experiments were then performed. The results of EdU assay, colony formation assay and transwell assay showed that overexpression of ULK1 could reverse the effect of circTMEM87A knockdown on cell proliferation and migration. Since ULK1 is associated with autophagy, we detected cellular autophagy by GFP/mRFP-LC3 puncta analysis, TEM and autophagy-related proteins expression detection. Emerging evidences suggested that autophagy could promote GC [39, 40]. We found knockdown of circTMEM87A reduced autophagy activity of GC cells and overexpression of ULK1 could reverse it. Autophagy can act as both tumor promoter and tumor suppressor in carcinogenesis [41, 42]. Autophagy acts as a barrier to tumor initiation while autophagy plays a positive role in cancer progression and maintenance after neoplastic lesions have been established [43]. During tumor progression, autophagy can provide substrates to help tumor cells overcome nutrient limitations and hypoxia [44]. In addition, inhibition of autophagy genes in tumor cells can induce cell death [45]. The results of our study also indicated that

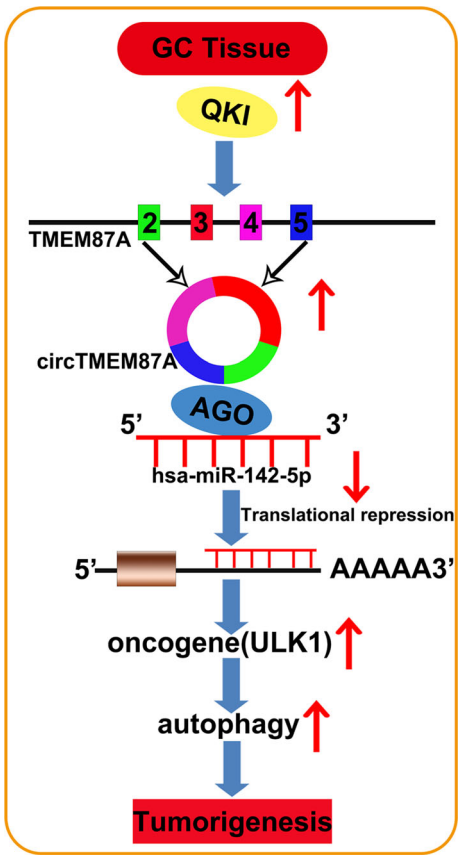

Fig. 7 The schematic diagram explaining the mechanism of oncogenic function of circTMEM87A Up-regulation of QKI promotes the formation of circTMEM87A in GC. CircTMEM87A sponges miR-142-5p to reduce the degradation effect of miR-142-5p on ULK1 mRNA. Up-regulation of ULK1 promotes autophagy and leads to tumorigenesis of GC

autophagy exerts a positive effect on gastric cancer progression. Expression of circTMEM87A was demonstrated to be positively associated with tumor weight of xenograft nude mice. We also proved the promotive effect of circTMEM87A on cell metastasis by in vivo bioluminescence imaging.

There were several limitations to this study. First, circulating circRNAs could serve as a better biomarker for diseases [46, 47], however, in this study circTMEM87A expression was only detected in GC tissues and cell lines rather than in plasma samples of GC patients. Second, the patients in this study received surgical operations about 3 years ago, so the long-term overall survival data are unavailable. The correlation between circTMEM87A expression and OS was analyzed on the base of 3-year survival. Third, whether circTMEM87A could exert its function by other mechanisms, such as binding to certain proteins was not elucidated. Forth, *Helicobacter pylori* (*H. pylori*) has been verified to be an important risk factor for GC [48]. Nevertheless, *H. pylori* examination is not a routine test for GC patients in our hospital, so we did not make a correlation analysis between *H. pylori* infection and circTMEM87A expression.

In conclusion, we confirmed that circTMEM87A could contribute to GC progression and could be regulated by QKI. We also elucidated that circTMEM87A functions by sponging miR-142-5p to up-regulate ULK1. The schematic diagram was shown in Fig. 7. These findings indicated that circTMEM87A might be a potential therapeutic target for GC.

Acknowledgements This work was supported by the National Natural Science Foundation of China (81871946, 81802917, 81902515); the Primary Research & Development Plan of Jiangsu Province (BE2016786); the Program for Development of Innovative Research Team in the First Affiliated Hospital of NJMU; the Priority Academic Program Development of Jiangsu Higher Education Institutions (PAPD, JX10231801); Jiangsu Key Medical Discipline (General Surgery) (ZDXKA2016005); and the Jiangsu Key Lab of Cancer Biomarkers, Prevention and Treatment, Collaborative Innovation Center for Cancer Personalized Medicine, Nanjing Medical University.

Author contributions HW and ZX contributed to the study conception and design. Material preparation, data collection and analysis were performed by HW, GS and PX. The first draft of the manuscript was written by HW and all authors commented on previous versions of the manuscript. All authors read and approved the final manuscript.

Compliance with ethical standards

Conflict of interest The authors declare that they have no conflict of interest.

References

1. Torre LA, Bray F, Siegel RL, et al. Global cancer statistics, 2012. CA Cancer J Clin. 2015;65:87–108.
2. Yang L. Incidence and mortality of gastric cancer in China. World J Gastroenterol. 2006;12:17–20.
3. Szasz AM, Lanczky A, Nagy A, et al. Cross-validation of survival associated biomarkers in gastric cancer using transcriptomic data of 1065 patients. Oncotarget. 2016;7:49322–33.
4. Catalano V, Labianca R, Beretta GD, et al. Gastric cancer. Crit Rev Oncol Hematol. 2009;71:127–64.
5. Wilusz JE, Sharp PA. A circuitous route to noncoding RNA. Science. 2013;340:440–1.
6. Jeck WR, Sorrentino JA, Wang K, et al. Circular RNAs are abundant, conserved, and associated with ALU repeats. RNA. 2013;19:141–57.
7. Szabo L, Morey R, Palpant NJ, et al. Statistically based splicing detection reveals neural enrichment and tissue-specific induction of circular RNA during human fetal development. Genome Biol. 2015;16:126.
8. Thomson DW, Dinger ME. Endogenous microRNA sponges: evidence and controversy. Nat Rev Genet. 2016;17:272–83.
9. Memczak S, Jens M, Elefsinioti A, et al. Circular RNAs are a large class of animal RNAs with regulatory potency. Nature. 2013;495:333–8.

10. Salzman J, Gawad C, Wang PL, et al. Circular RNAs are the predominant transcript isoform from hundreds of human genes in diverse cell types. PLoS ONE. 2012;7:e30733.
11. Li Y, Zheng F, Xiao X, et al. CircHIPK3 sponges miR-558 to suppress heparanase expression in bladder cancer cells. EMBO Rep. 2017;18:1646–59.
12. Qu S, Zhong Y, Shang R, et al. The emerging landscape of circular RNA in life processes. RNA Biol. 2017;14:992–9.
13. Hansen TB, Jensen TI, Clausen BH, et al. Natural RNA circles function as efficient microRNA sponges. Nature. 2013;495:384–8.
14. Han D, Li J, Wang H, et al. Circular RNA circMTO1 acts as the sponge of MicroRNA-9 to suppress hepatocellular carcinoma progression. Hepatology. 2017;66:1151–64.
15. Chen L, Zhang S, Wu J, et al. circRNA_100290 plays a role in oral cancer by functioning as a sponge of the miR-29 family. Oncogene. 2017;36:4551–61.
16. Hsiao KY, Lin YC, Gupta SK, et al. Noncoding effects of circular RNA CCDC66 promote colon cancer growth and metastasis. Cancer Res. 2017;77:2339–50.
17. Sun G, Li Z, Wang W, et al. miR-324-3p promotes gastric cancer development by activating Smad4-mediated Wnt/beta-catenin signaling pathway. J Gastroenterol. 2018;53:725–39.
18. Ebert MS, Sharp PA. Roles for microRNAs in conferring robustness to biological processes. Cell. 2012;149:515–24.
19. Bartel DP. MicroRNAs: genomics, biogenesis, mechanism, and function. Cell. 2004;116:281–97.
20. Yan J, Yang B, Lin S, et al. Downregulation of miR-142-5p promotes tumor metastasis through directly regulating CYR61 expression in gastric cancer. Gastric Cancer. 2019;22:302–13.
21. Wang Z, Liu Z, Fang X, et al. MiR-142-5p Suppresses Tumorigenesis by Targeting PIK3CA in Non-Small Cell Lung Cancer. Cell Physiol Biochem. 2017;43:2505–15.
22. Mizushima N, Komatsu M. Autophagy: renovation of cells and tissues. Cell. 2011;147:728–41.
23. Kimmelman AC. The dynamic nature of autophagy in cancer. Genes Dev. 2011;25:1999–2010.
24. Mathew R, Karantza-Wadsworth V, White E. Role of autophagy in cancer. Nat Rev Cancer. 2007;7:961–7.
25. Zhu X, Yang G, Xu J, et al. Silencing of SNHG6 induced cell autophagy by targeting miR-26a-5p/ULK1 signaling pathway in human osteosarcoma. Cancer Cell Int. 2019;19:82.
26. Chen MB, Ji XZ, Liu YY, et al. Ulk1 over-expression in human gastric cancer is correlated with patients' T classification and cancer relapse. Oncotarget. 2017;8:33704–12.
27. Conn SJ, Pillman KA, Toubia J, et al. The RNA binding protein quaking regulates formation of circRNAs. Cell. 2015;160:1125–34.
28. Ivanov A, Memczak S, Wyler E, et al. Analysis of intron sequences reveals hallmarks of circular RNA biogenesis in animals. Cell Rep. 2015;10:170–7.
29. Aktaş T, Avşar Ilık İ, Maticzka D, et al. DHX9 suppresses RNA processing defects originating from the Alu invasion of the human genome. Nature. 2017;544:115–9.
30. White E, Mehnert JM, Chan CS. Autophagy, metabolism, and cancer. Clin Cancer Res. 2015;21:5037–46.
31. Nie Y, Wu K, Yu J, et al. A global burden of gastric cancer: the major impact of China. Expert Rev Gastroenterol Hepatol. 2017;11:651–61.
32. Dong Y, He D, Peng Z, et al. Circular RNAs in cancer: an emerging key player. J Hematol Oncol. 2017;10:2.
33. Yao R, Xu L, Wei B, et al. miR-142-5p regulates pancreatic cancer cell proliferation and apoptosis by regulation of RAP1A. Pathol Res Pract. 2019;215:152416.
34. Islam F, Gopalan V, Vider J, et al. MiR-142-5p act as an oncogenic microRNA in colorectal cancer: clinicopathological and functional insights. Exp Mol Pathol. 2018;104:98–107.
35. Yu W, Li D, Zhang Y, et al. MiR-142-5p acts as a significant regulator through promoting proliferation, invasion, and migration in breast cancer modulated by targeting SORBS1. Technol Cancer Res Treat. 2019;18:1533033819892264.
36. Li M, Cai O, Tan S. LOXL1-AS1 drives the progression of gastric cancer via regulating miR-142-5p/PIK3CA axis. Onco Targets Ther. 2019;12:11345–57.
37. Zhang X, Yan Z, Zhang J, et al. Combination of hsa-miR-375 and hsa-miR-142-5p as a predictor for recurrence risk in gastric cancer patients following surgical resection. Ann Oncol. 2011;22:2257–66.
38. Wang B, Iyengar R, Li-Harms X, et al. The autophagy-inducing kinases, ULK1 and ULK2, regulate axon guidance in the developing mouse forebrain via a noncanonical pathway. Autophagy. 2018;14:796–811.
39. Xu Z, Li Z, Wang W, et al. MIR-1265 regulates cellular proliferation and apoptosis by targeting calcium binding protein 39 in gastric cancer and thereby, impairing oncogenic autophagy. Cancer Lett. 2019;449:226–36.
40. Kong P, Zhu X, Geng Q, et al. The microRNA-423-3p-Bim axis promotes cancer progression and activates oncogenic autophagy in gastric cancer. Mol Ther. 2017;25:1027–37.
41. Zhou H, Yuan M, Yu Q, et al. Autophagy regulation and its role in gastric cancer and colorectal cancer. Cancer Biomark. 2016;17:1–10.
42. Singh SS, Vats S, Chia AY, et al. Dual role of autophagy in hallmarks of cancer. Oncogene. 2018;37:1142–58.
43. Katheder NS, Khezri R, O'Farrell F, et al. Microenvironmental autophagy promotes tumour growth. Nature. 2017;541:417–20.
44. Chen P, Cescon M, Bonaldo P. Autophagy-mediated regulation of macrophages and its applications for cancer. Autophagy. 2014;10:192–200.
45. Chang Y, Yan W, He X, et al. miR-375 inhibits autophagy and reduces viability of hepatocellular carcinoma cells under hypoxic conditions. Gastroenterology. 2012;143(177–87):e8.
46. Hang D, Zhou J, Qin N, et al. A novel plasma circular RNA circFARSA is a potential biomarker for non-small cell lung cancer. Cancer Med. 2018;7:2783–91.
47. Zhang J, Xu Y, Xu S, et al. Plasma circular RNAs, Hsa_circRNA_025016, predict postoperative atrial fibrillation after isolated off-pump coronary artery bypass grafting. J Am Heart Assoc. 2018;7:e006642.
48. Amieva M, Peek RM Jr. Pathobiology of Helicobacter pylori-induced gastric cancer. Gastroenterology. 2016;150:64–78.